

Electron-impact ionization of argon $3p$ in asymmetric kinematicsK. Bechane ¹, S. Houamer ^{1,*}, T. Khatir ^{1,2}, A. Tamin ¹ and C. Dal Cappello³¹*LPQSD, Department of Physics, Faculty of Sciences, University Sétif 1, Sétif 19000, Algeria*²*CRNA, 02, Boulevard Frantz Fanon, Boîte Postale 399, Alger RP, Algeria*³*LPCT, UMR CNRS 7019, University of Lorraine, Boîte Postale 95823, 57078 METZ Cedex3, France*

(Received 7 September 2023; revised 1 November 2023; accepted 19 December 2023; published 19 January 2024)

Triple differential cross sections are presented for the electron impact ionization of a $3p$ shell of argon, using a model called 3CWZ. Within this model, the projectile as well as the ejected electrons are represented by Coulomb waves with variable charges $Z(r)$ instead of an effective charge; the postcollision interaction (PCI) is also included and treated exactly at all orders of perturbation theory. Our results are compared with recent experiments and other theoretical predictions in a range of several kinematics.

DOI: [10.1103/PhysRevA.109.012812](https://doi.org/10.1103/PhysRevA.109.012812)**I. INTRODUCTION**

Electron impact ionization of atoms and molecules represents theoretically a few-body problem which remains still unresolved since the Schrödinger equation cannot be analytically solvable for more than two interacting particles. There has been, however, impressive progress in theoretical studies, especially with the emergence of new generations of experiences allowing one to probe the validity of any theory. Experimentally, coincidence techniques have allowed for complete information about all particles, and are currently widely used to investigate the electronic structure of the targets besides the fundamental interactions involved in the reaction. These coincidence experiments, also called ($e, 2e$) reactions [1–3], provide the most valuable information of the reaction and constitute a real challenging test for theories; in particular, the measured triple differential cross section (TDCS) represents a rigorous test for the most efficient models. Accordingly, advanced theoretical studies have been carried out from the early days in response to the discrepancies observed between theory and experiments. The history of this three-body problem is rather long and rich; a detailed description of theoretical models developed gradually to investigate the ionization reaction can be found in [4]. We briefly recall here some efficient models which are nowadays known to provide the best description of the ($e, 2e$) reaction; these models could hence represent a good tool of comparison for any theoretical study like that we propose in this work. The distorted wave Born approximation (DWBA), where the continuum electrons are all represented by distorted waves, has been proven to be one of the most successful models in describing ($e, 2e$) experiments for multielectron targets [5–8]. The model does not take into account the PCI; its advantage lies, however, in the simplicity of including the different contributions to the ionization process such as exchange and distortion effects. The DWBA model was refined and

extended for the first time by Prideaux and Madison to atoms [9] by including the PCI in the final state and was generalized later for molecules [10,11]. As a result any physics contained in the wave function is contained to all orders of perturbation theory; this modeling was called 3DW for atoms and M3DW for molecules. Overall, the model has been successfully applied and has given good predictions of the triple differential cross section [12–14]. A hybrid approach based upon DWBA and the R -matrix [15] models has also been developed; this description treats the many-electron process in the ionized target in a more elaborate way than that used in the DWBA model. Theoretical calculations were primarily first-order R matrix [16,17] and extended to second-order R matrix [18,19]; the models are called DWB1-RM and DWB2-RM, respectively. Rather sophisticated nonperturbative models were also developed, following the impressive development of computer resources such as the CCC [20,21] and BSR [22,23] models. In the CCC (convergent close-coupling) approximation, the total wave function is expanded in terms of a sum of products of the target Hamiltonian eigenstates and unknown wave functions related to the projectile; these unknown wave functions are determined by solving a system of integro-differential equations. Besides, the R -matrix method is based on the partition of the configuration space into inner and outer regions; the wave function of the target is required to be totally contained within this inner region. The BSR method is based upon a two-step treatment: (i) the method uses the nonperturbative close-coupling expansion, and (ii) the close-coupling equations are solved using the R -matrix method. There has been significant progress in experimental ($e, 2e$) techniques which have allowed for complete kinematic information since the first measurements of Jung *et al.* [24] followed over the years by no-less-valuable works which provided additional insight into the ionization process [25–27]. Further techniques have emerged since then, such as the COLd-target recoil-ion momentum spectroscopy technique (COLTRIMS) which was developed during the late 1980s and which contributed extensively in the development of the coincidence measurements [28]; this new technique has allowed researchers to perform

*s_houamer@univ-setif.dz

kinematically complete experiments involving photons, ions, and electrons. While molecular targets have been investigated with limited theoretical support due to their multicenter character as well as to computation time constraints, considerable attention has been given to atoms for a long time. As a result, $(e, 2e)$ measurements can now be correctly predicted for light atoms like hydrogen and helium by sophisticated models [29]. However, for more complex atoms the agreement is not automatically as good; in particular, argon has proven to present a great challenge for theory [30]. Further investigations in this respect are then called for to clarify the origin of the observed discrepancies between theory and experiment. There have been many experiments devoted to the ionization of argon atoms in several kinematics where relative as well as absolute measurements have been provided [31–33]. It should be noted that in almost cases, studies were restricted to coplanar geometry which was admitted to contain the relevant physics of the process (in the coplanar geometry, the incoming projectile and the outgoing electrons are detected in a common plane called the scattering plane). With the appearance of new techniques like those using an advanced reaction microscope, where a nearly full solid angle data collection can be achieved, more valuable information about the $(e, 2e)$ process can now be provided, in many kinematics [34]. Our aim in this work is to further investigate the ionization of argon $3p$ using a theoretical approach in various kinematics.

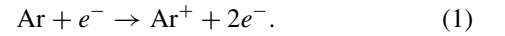
In a previous work [35], we presented a model called BBK2CWZ1, where the two outgoing electrons were described by Coulomb waves with variable charges while the incoming electron was represented by a plane wave; this was considered as an improved BBK model. The model was applied successfully to some atomic and (the Brauner, Briggs and Klar (BBK) model is defined and discussed in [35] and references therein) molecular targets at intermediate and high

impact energies where the use of a plane wave for the incoming electron is justified; an overall improvement in the agreement with measurements was observed compared to the standard BBK results. In this work we improve our modeling by representing all the continuum electrons by Coulomb waves with variable charges or, in other words, the incoming electron will be described now by a Coulomb wave instead of a plane wave as was done in [35]. This model called 3CWZ, which is expected to constitute a more elaborate approach to the $(e, 2e)$ reaction than BBK2CWZ1, is applied at intermediate and low impact energies. We will focus basically on the ionization of argon $3p$ by electron impact because it is the most extensively studied many-electron system and for which rather valuable experiments have been performed.

The paper is organized as follows: the theoretical model is outlined in the next section. Our results are presented and discussed in the third section. We finish by a Conclusion and outlook. Atomic units are used throughout, unless specified otherwise.

II. THEORY

The electron impact ionization of an argon atom in its ground state is schematized as



The theoretical background of the $(e, 2e)$ process can be found in our former works [35–37]. In this work we take into account the exchange effects which were omitted previously as we considered only highly asymmetric coplanar geometric kinematics and relatively high impact energy. Briefly, in the single-particle picture, the triple differential cross section of an atomic subshell (n, l, m) is written, after summing over all final and averaging over all initial spin states, as [4]

$$\sigma^{(3)} = \frac{d^3\sigma}{d\Omega_1 d\Omega_2 dE_1} = (2\pi)^4 \frac{k_1 k_2}{k_i} (|T_{\text{dir}}|^2 + |T_{\text{exc}}|^2 + |T_{\text{dir}} - T_{\text{exc}}|^2). \quad (2)$$

The transition matrix elements T_{dir} and T_{exc} are given by

$$T_{\text{dir}} = \left\langle \phi_c^Z(\vec{k}_1, \vec{r}_0) \phi_c^Z(\vec{k}_2, \vec{r}_1) C(\alpha_{01}, \vec{k}_{01}, \vec{r}_{01}) \left| \frac{1}{r_{01}} - \frac{1}{r_0} \right| \phi_c^Z(\vec{k}_i, \vec{r}_0) \Psi_{nlm}(\vec{r}_1) \right\rangle, \quad (3)$$

$$T_{\text{exc}} = \left\langle \phi_c^Z(\vec{k}_1, \vec{r}_1) \phi_c^Z(\vec{k}_2, \vec{r}_0) C(\alpha_{01}, \vec{k}_{01}, \vec{r}_{01}) \left| \frac{1}{r_{01}} - \frac{1}{r_0} \right| \phi_c^Z(\vec{k}_i, \vec{r}_0) \Psi_{nlm}(\vec{r}_1) \right\rangle, \quad (4)$$

where \vec{k}_i , \vec{k}_1 , and \vec{k}_2 are, respectively, the momentum vectors of the incident, scattered, and ejected electrons while $\phi_c^Z(\vec{k}, \vec{r})$ represents a Coulomb wave with variable charge $Z(r)$:

$$\phi_c^Z(\vec{k}, \vec{r}) = \frac{\exp(i\vec{k} \cdot \vec{r})}{(2\pi)^{3/2}} {}_1F_1 \left[-i \frac{Z(r)}{k}, 1, -i(\vec{k} \cdot \vec{r} + \vec{k}r) \right] \exp \left[\frac{\pi Z(r)}{2k} \right] \Gamma \left[1 + i \frac{Z(r)}{k} \right]. \quad (5)$$

$C(\alpha_{01}, \vec{k}_{01}, \vec{r}_{01})$ is the full final Coulomb interaction dealing with the PCI and is given by

$$C(\alpha_{01}, \vec{k}_{01}, \vec{r}_{01}) = \exp \left(-\frac{\pi}{4k_{01}} \right) \Gamma \left(1 - \frac{i}{2k_{01}} \right) {}_1F_1 \left[-i\alpha_{01}, 1, -i(\vec{k}_{01} \cdot \vec{r}_{01} + k_{01}r_{01}) \right], \quad (6)$$

with $\vec{k}_{01} = \frac{1}{2}(\vec{k}_0 - \vec{k}_1)$ and $\alpha_{01} = -\frac{1}{2k_{01}}$.

$\Psi_{nlm}(\vec{r})$ is the bound wave function of the atomic target, expanded in the Roothaan-Hartree-Fock method as a linear combination of Slater-type wave functions [38].

The momentum vectors are required to fulfill the conservation law $\vec{q} = \vec{K} - \vec{k}_2$, where \vec{q} is the recoil momentum and $\vec{K} = \vec{k}_i - \vec{k}_1$ is the momentum transfer.

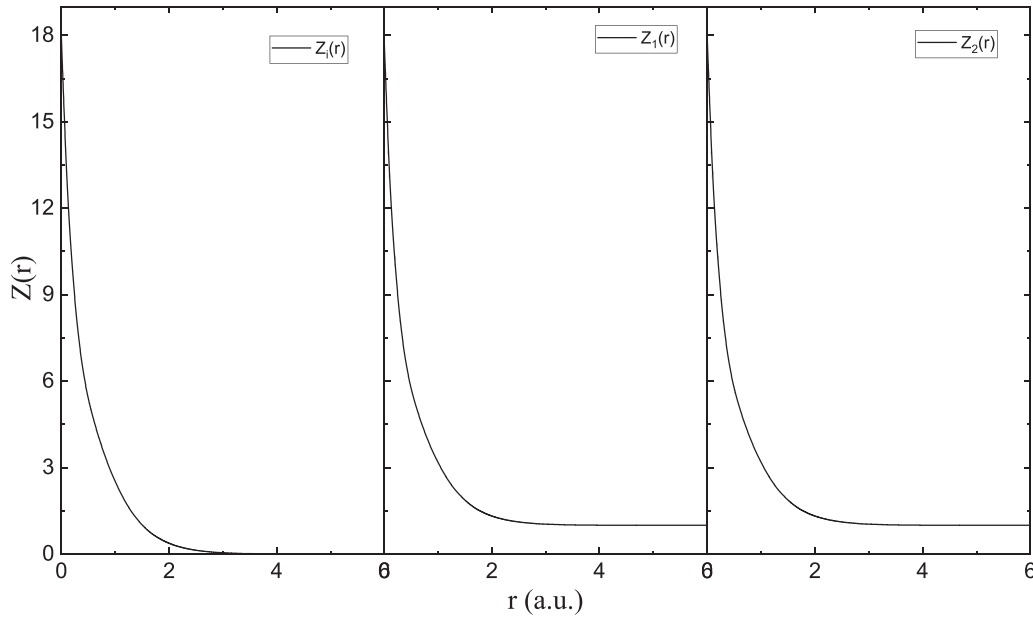


FIG. 1. Variable charge $Z(r)$ seen by the incident electron (a), the ejected electron (b), and the scattered electron (c) during the ionization process for the 3*p* subshell of Ar.

The variable charge is calculated analytically by using the spherically averaged potential of the target viewed by the electron:

$$U_i(r_1) = \frac{1}{4\pi} \int V_i(\vec{r}_1) d\Omega_1 = -\frac{Z(r_1)}{r_1}, \quad (7)$$

where $V_i(\vec{r}_1)$ is the standard Hartree potential defined for atoms by

$$V_i(\vec{r}_1) = -\frac{Z}{r_1} + \sum_{i=1}^{N_0} N_{ij} \int \frac{|\phi_j(\vec{r})|^2}{|\vec{r} - \vec{r}_1|} d\vec{r}. \quad (8)$$

In our modeling the ejected and scattered electrons see a charge $Z = N$ at the center of the target and $Z = 1$ asymptotically, while the incident electron sees a charge $Z = N$ at the center and $Z = 0$ asymptotically. These variable charges are called $Z_i(r)$, $Z_1(r)$, and $Z_2(r)$ for the incident, scattered, and ejected electron, respectively. In Fig. 1 we present the variable charges for the ionization of argon 3*p*; the three panels display $Z(r)$ corresponding to the continuum electrons. One can clearly see that $Z_1(r)$ and $Z_2(r)$ decrease from $Z = 18$ to $Z = 1$ whereas $Z_i(r)$ decreases from $Z = 18$ to $Z = 0$; the asymptotic values of $Z(r)$ are reached rapidly at a distance of about $r = 3$ au. It is worth noting that the validity of using the variable charge modeling in our treatment has been discussed and justified in our previous work [35] by performing a partial wave comparative analysis between a true distorted wave and a spherical Coulomb wave with variable charge. To further check the validity of our present analysis, we make a comparison between the static potential used here to deduce the variable charge with the full distorting potential of the DWBA model. The full distorting potential is written as

$$U(r) = V_{\text{stat}}(r) + V_{\text{ex}}(r) + V_p(r), \quad (9)$$

where the local exchange $V_{\text{ex}}(r)$ and polarization $V_p(r)$ potentials are widely used in collision theory and their expressions

are well known (see [39] for $V_{\text{ex}}(r)$ and [40] or $V_p(r)$). The variable charge $Z(r)$ has been calculated by keeping only $V_{\text{stat}}(r)$ in Eq. (9), which is actually written as $V_{\text{stat}}(r) = -\frac{Z(r)}{r}$. For comparison purposes, the radial distribution of the static potential $V_{\text{stat}}(r)$ as well as the full distorting potential $U(r)$ are displayed in Fig. 2. It is seen that the two potentials exhibit somewhat the same shape and could be considered roughly similar. The most notable differences are observed in the short range region, while the two potentials are practically the same elsewhere; thereby the approach used in this work to calculate the variable charge appears to be fairly reasonable.

The object of this work concerns the use of this variable charge modeling, which somehow represents a full approximate distorted wave model (a kind of a 3DW model), and to check how this will affect the TDCS in the (*e*, 2*e*) reaction of argon 3*p* by considering several kinematics. The model

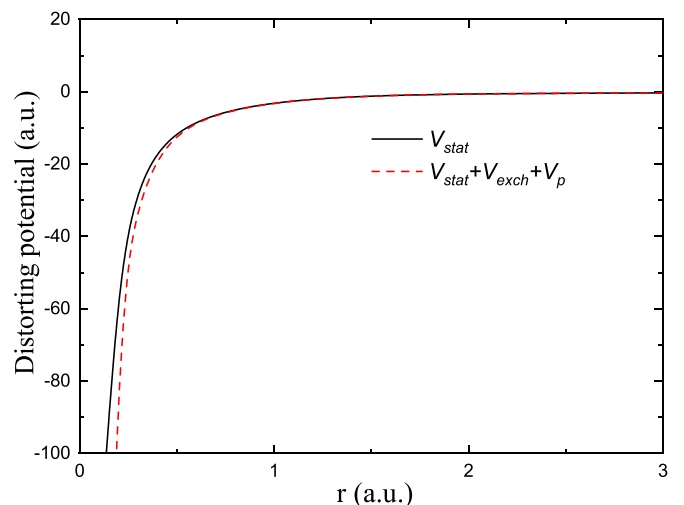


FIG. 2. Distorting potential $U(r)$ seen by the ejected electron.

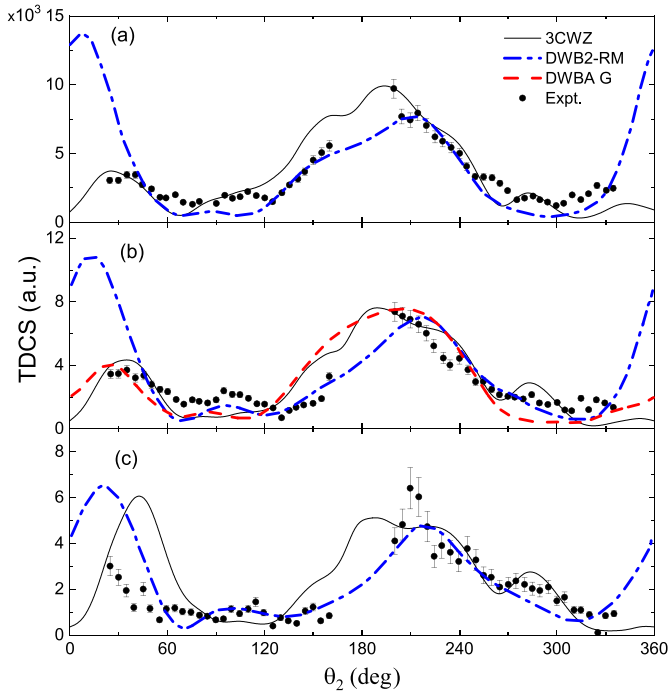


FIG. 3. TDCS for the ionization of argon $3p$ as a function of the ejection angle θ_2 at fixed scattering and ejected energies $E_1 = 500$ eV and $E_2 = 205$ eV. The projectile is scattered at a fixed scattering angle (a) $\theta_1 = 3^\circ$, (b) $\theta_1 = 6^\circ$, and (c) $\theta_1 = 9^\circ$. Theoretical results are black solid line (3CWZ), red dashed line (DWBA-G) and blue dash-dot line (DWB2-RM). The experimental data are black circles taken from [41]. The data have been normalized for the best visual agreement with theory. The absolute scale shown is that of the 3CWZ calculations. The DWB2-RM results have been multiplied by 0.34 (a), 0.33 (b), and 0.25 (c). The DWBA-G results have been multiplied by 1.34 (b).

is called 3CWZ; the obtained results within this model are compared with experiments and other theories. We would like to note that the evaluation of matrix elements (3) and (4) requires great care; we used in this work a Fourier transform scheme to carry out calculations in a rather convenient way (see, e.g., [37], and references therein).

III. RESULTS

We have calculated the TDCS for the ionization of the argon $3p$ subshell using the 3CWZ model; obtained results are now presented and discussed by considering several kinematics in asymmetric geometries. Figure 3 exhibits calculated TDCSs in coplanar asymmetric geometry at an incident energy of about 721 eV and an ejected energy of 205 eV. Three sets of experimental data performed for three scattered angles $\theta_1 = 3^\circ$, 6° , and 9° display the TDCS as a function of the ejection angle. Our results are compared with experiments [41] as well as DWB2-RM and DWBA-G theoretical models. Since experiments are given on a relative scale, we normalize the data as well as the theoretical calculations to the 3CWZ model. These kinematics are characterized by large momentum transfer ($K = 1.27$, 1.4 , and 1.6 a.u.) and large recoil momentum absorbed by the atom (q up to 5.48 a.u.)

which indicates that the recoil ion participates strongly in the reaction which would require a rigorous modeling of the ionization process. Also, in this particular situation the PCI is expected to strongly affect the TDCS as the ejected and scattered energies are rather close to each other. We should note that BBK has already proven to fail completely in describing the recoil region of the TDCS [35]; more sophisticated models are therefore needed for the study of the reaction dynamics for these particular kinematics. Looking at Fig. 3 in detail, it is seen that overall the DWB2-RM model describes many parts of the TDCS well but exhibits in all cases a binary peak significantly larger than that of the recoil region, in clear contradiction with the data. Besides, it can be observed that 3CWZ is able to reproduce quite well the TDCS in most parts of the angular distribution of the TDCS; in particular, the peaks in the binary and the recoil regions are much better described compared to those of DWB2-RM. On the other hand it is seen that DWBA-G [42] (for which only results for $\theta_1 = 6^\circ$ are available) provides results rather closer to experiments like those of 3CWZ [panel (b)]. To give an interpretation of these findings we recall that DWB2-RM is a powerful model which is in principle able to generally well describe the $(e, 2e)$ reaction. Nevertheless this model does not account for the PCI, which is important here; this explains unfortunately the shortcomings observed in Fig. 3. In contrast, the DWBA-G model is a full distorted wave model where the PCI is included via the Gamow factor. This model is in fact not convenient for comparison with absolute measurements, as the Gamow factor is known to violate strongly the normalization, but can be efficient for comparison with relative data like those considered here. The failure of the DWB2-RM model to correctly predict some regions of the TDCS highlights the importance of the PCI effect, which is not accounted for within this model for these particular kinematics. Furthermore, 3CWZ is a kind of an approximate full distorted wave approach with PCI; the spherical static potential which enables resolving the Schrödinger equation in the true distorted wave description is used instead to calculate the variable charge $Z(r)$ in the 3CWZ model.

In the following we investigate the case of lower impact energy and lower momentum transfer where theoretical calculations are now compared with absolute data [30]. Figure 4 shows a comparison between 3CWZ results with the absolute data at 200 and 113.5 eV impact energies, respectively; also included are the theoretical predictions of the 3DW, DWBA, and DWB2-RM models. Looking at the figure in detail, it is seen that unfortunately none of the theoretical models is able to correctly reproduce the magnitude of the TDCS. It is overall observed that 3CWZ reproduces the double peak in the binary region qualitatively well; the second binary peak is, however, larger than the first one in all kinematics. At 200 eV impact energy [panels (a) and (b)], we can already see that the absolute data are underestimated by all theories. It is, however, observed that 3CWZ reproduces quite well the double binary peak; we also note that the 3CWZ results are rather close to those of DWB2-RM in the binary region while DWBA and 3DW predict nearly the same shape and magnitude for the TDCS. Surprisingly, 3DW, which represents in principle a rather sophisticated modeling of the process, does not reproduce the double binary peak [panel (a)] as would

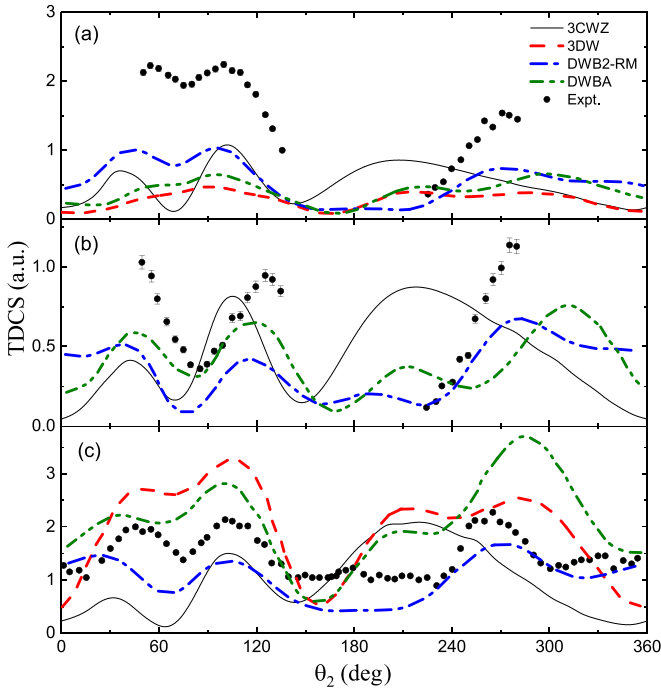


FIG. 4. Absolute TDCS for the ionization of argon 3*p* as a function of the ejection angle θ_2 at fixed scattering angle $\theta_1 = 15^\circ$. The incident and ejected electrons have respective energies (a) $E_i = 200$ eV and $E_2 = 10$ eV, (b) $E_i = 200$ eV and $E_2 = 5$ eV, and (c) $E_i = 113.5$ eV and $E_2 = 5$ eV. Theoretical results are black solid line (3CWZ), red dashed line (3DW), blue dash-dot line (DWB2-RM), and green dash-dot-dot line (DWBA). The experimental data are black circles taken from [30].

be expected. DWBA exhibits somewhat the same behavior as 3DW at $E_2 = 10$ eV [panel (a)]; it reproduces nevertheless the double binary peak at $E_2 = 5$ eV [panel (b)]. The same trends are still observed at 113.5 eV projectile energy, noting anyway that in the present case the absolute data are much closer to all theories. Furthermore, it should be indicated that the data are underestimated by 3CWZ and DWB2-RM, whereas 3DW and DWBA predict much higher intensities [panel (c)]. Also seen, 3CWZ results are closer to those of DWB2-RM as was observed for 200 eV impact energy. In the recoil region, none of the theoretical models is able to correctly reproduce the data.

To summarize discussion of Fig. 4, we can state that the 3CWZ model does not correctly describe the absolute data but qualitatively reproduces the shape of the TDCS in the binary region. We nevertheless note that 3CWZ provides results which are at least at the same level of agreement with experiments as other highly developed models. Overall, 3CWZ as well as all theories considered in this work, provides results whose agreement with experiments is somewhat mixed; no competition between theories is visible for these kinematics. More extensive studies would likely allow us to gain deep insight into the ionization reaction.

Lastly, in order to get more insight into the dynamics of the (*e*, 2*e*) reaction, we are interested in the study of the ionization reaction at 195 eV impact energy where experiments have been performed using an efficient reaction microscope

especially designed for electron impact experiments [34]. It is worth noting that the coplanar geometry was used for a long time in (*e*, 2*e*) studies as it was assumed to contain most of the relevant physics of the reaction, while experiments investigating out-of-plane geometries remained scarce [43]. The novelty is that the measured TDCSs in this new generation of experiences cover a large part of the full solid angle of the ejected electrons; these ejected electrons are detected outside the scattering plane with energies that can reach 25 eV, representing thereby a new challenge for theory. Accordingly, new kinematics are given beyond the coplanar geometry, which allows one to provide comprehensive information of the ionization dynamics. A three-dimensional TDCS image is therefore given as a function of the emission solid angle (θ_2, ϕ_2) for a particular value of the scattering angle θ_1 . For more valuable comparisons, TDCS cuts in three orthogonal planes are given; these cuts correspond to the *xz* plane (scattering plane), the *yz* plane (half-perpendicular plane), and the *xy* plane (full-perpendicular plane).

Our study is focused in the following on the electron impact ionization of argon 3*p* at 195 eV impact energies for fixed scattering angles ranging from $\theta_1 = 5^\circ$ to $\theta_1 = 20^\circ$. The results are displayed in Figs. 5–7 for three ejection energies of 10 eV, 15, and 20 eV, respectively. The interesting aspect of the present study lies in the fact that the experiments are given on an absolute scale [44] which would provide a benchmark for comparison with theory.

Figure 5 shows absolute TDCS cuts in the three perpendicular planes for an ejection energy $E_2 = 10$ eV (the convention adopted here is so that $\phi_2 = 0$ corresponds to the *x* axis). The cross sections in the *xz*, *yz*, and *xy* planes are displayed as a function of the ejected angle for a set of scattering angles $\theta_1 = 5^\circ, 10^\circ, 15^\circ$, and 20° ; 3CWZ results are then compared with experiments as well as DWB2-RM predictions. In the scattering plane (left-hand column) it is shown that, overall, the 3CWZ model predicts the data quite well; the model reproduces the binary peak of the TDCS for $\theta_1 = 5^\circ$ very well, but agreement becomes less good with increasing scattering angles (and then increasing momentum transfer). We also note that the binary peak observed for $\theta_1 = 5^\circ$ splits in two with increasing scattering angles in agreement with the data; it is well known that this double peak structure is attributed to the *p* character of the outer shell of argon. When we compare with the DWB2-RM results, it is seen that the 3CWZ model tends to better describe the (*e*, 2*e*) process than DWB2-RM, especially for higher scattering angles $\theta_1 = 15^\circ$ and 20° ; also the double peak structure for higher scattering angles is better exhibited by the 3CWZ model. We should note anyway that the recoil peak is shifted to lower angles by 3CWZ. When we consider the *yz* plane (central column) we can already see that the data are symmetric about 180° ; the DWB2-RM model reproduces the whole shape of the TDCS much better while 3CWZ exhibits a strong recoil peak in all cases. The binary region is not correctly reproduced by 3CWZ except for $\theta_1 = 5^\circ$ where a binary peak close to experiments is visible. Overall, the DWB2-RM model better describes the shape of the peaks in the binary and recoil regions, significant discrepancies in magnitude with the data are unfortunately observed. In the *xy* plane (right-hand column), it is seen overall that the agreement with experiments is somewhat mixed when we look in detail

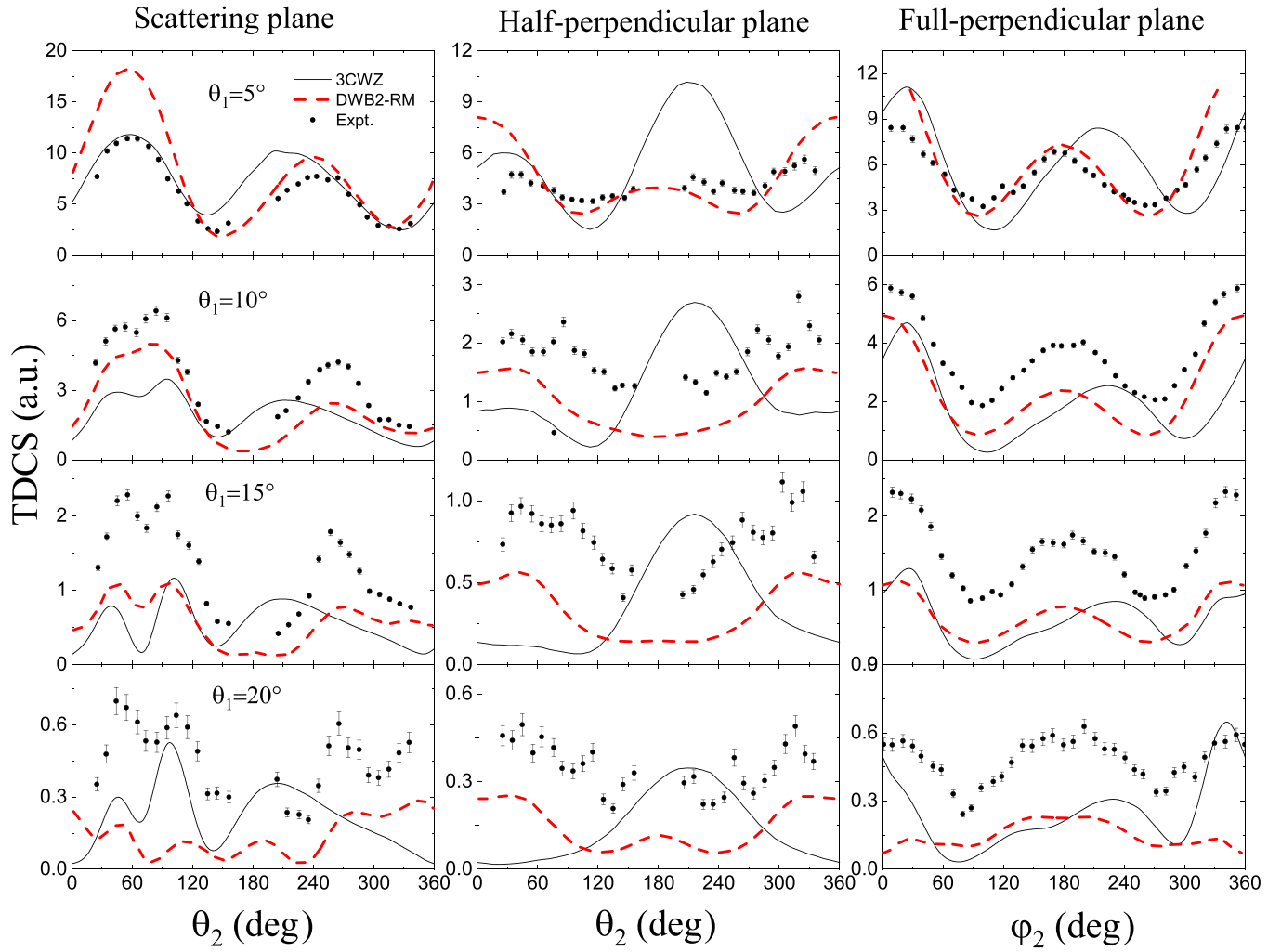


FIG. 5. Absolute TDCS (presented as cuts of the 3D image) for the ionization of argon $3p$ by an impact energy $E_i = 195$ eV as a function of the ejection solid angle (θ_2, ϕ_2). The projectile is scattered at angles $\theta_1 = (5^\circ, 10^\circ, 15^\circ, 20^\circ)$ in coincidence with the ejected electron with an energy $E_2 = 10$ eV. Left-hand column: TDCS in scattering (xz) plane. Central column: TDCS in the half-perpendicular (yz) plane. Right-hand column: TDCS in the full-perpendicular (xy) plane. Theoretical results are black solid line (3CWZ) and red dashed line (DWB2-RM). The experimental data are black circles taken from [44].

at the TDCSs provided by the 3CWZ and DWB2-RM models. The DWB2-RM model seems to better reproduce the TDCS for these kinematics ($E_2 = 10$ eV); the agreement with the data is quite good at low scattering angles (5° and 10°). However, this good agreement is no longer observed with increasing scattering angles where the data are substantially underestimated (by a factor up to 2); the agreement becomes even better reproduced by 3CWZ at a 20° scattering angle.

Figures 6 and 7 show the absolute TDCSs with the same set of scattering angles but for ejection energies $E_2 = 15$ and 20 eV, respectively. Our theoretical results are compared with experiments as well as those of the DWB2-RM model once again; general trends observed are quite similar to those of Fig. 5. As seen, the TDCS is qualitatively reproduced by the two models in the xz plane where the double peak structure is still shown for higher angles, in agreement with experiments. The 3CWZ model still provides a better description of the absolute TDCS, especially at $\theta_1 = 20^\circ$. In the half-perpendicular plane (yz plane) DWB2-RM is better at reproducing the shape of the TDCS where the binary and recoil peaks are still

qualitatively reproduced; the magnitude of the TDCS is nevertheless substantially underestimated for all scattering angles. The 3CWZ results are also in worse agreement compared to DWB2-RM; the binary peak is somewhat more visible for these two energies (better than for $E_2 = 10$ eV) and a large recoil peak is reproduced too. The situation is different for the xy plane: the 3CWZ model better describes the TDCS in shape and magnitude, and a peak at about $\phi_2 = 20^\circ$ is observed for all scattering angles. On the other hand, DWB2-RM does not reproduce the data, especially at higher scattering angles, $\theta_1 = 15^\circ$ and 20° , where clear discrepancies are observed.

It should be noted that DWB2-RM is *a priori* a more sophisticated treatment as it uses accurate multiconfiguration expansion of the final ionic states as well as the initial bound state instead of a single-configuration scheme; the observed shortcomings are presumably due to the fact that the PCI is not accounted for at all for this model. In contrast, 3CWZ appears to reproduce the data quite well in many cases, at least for this intermediate impact energy (195 eV), although it is based on a rather simple modeling. This indicates the importance

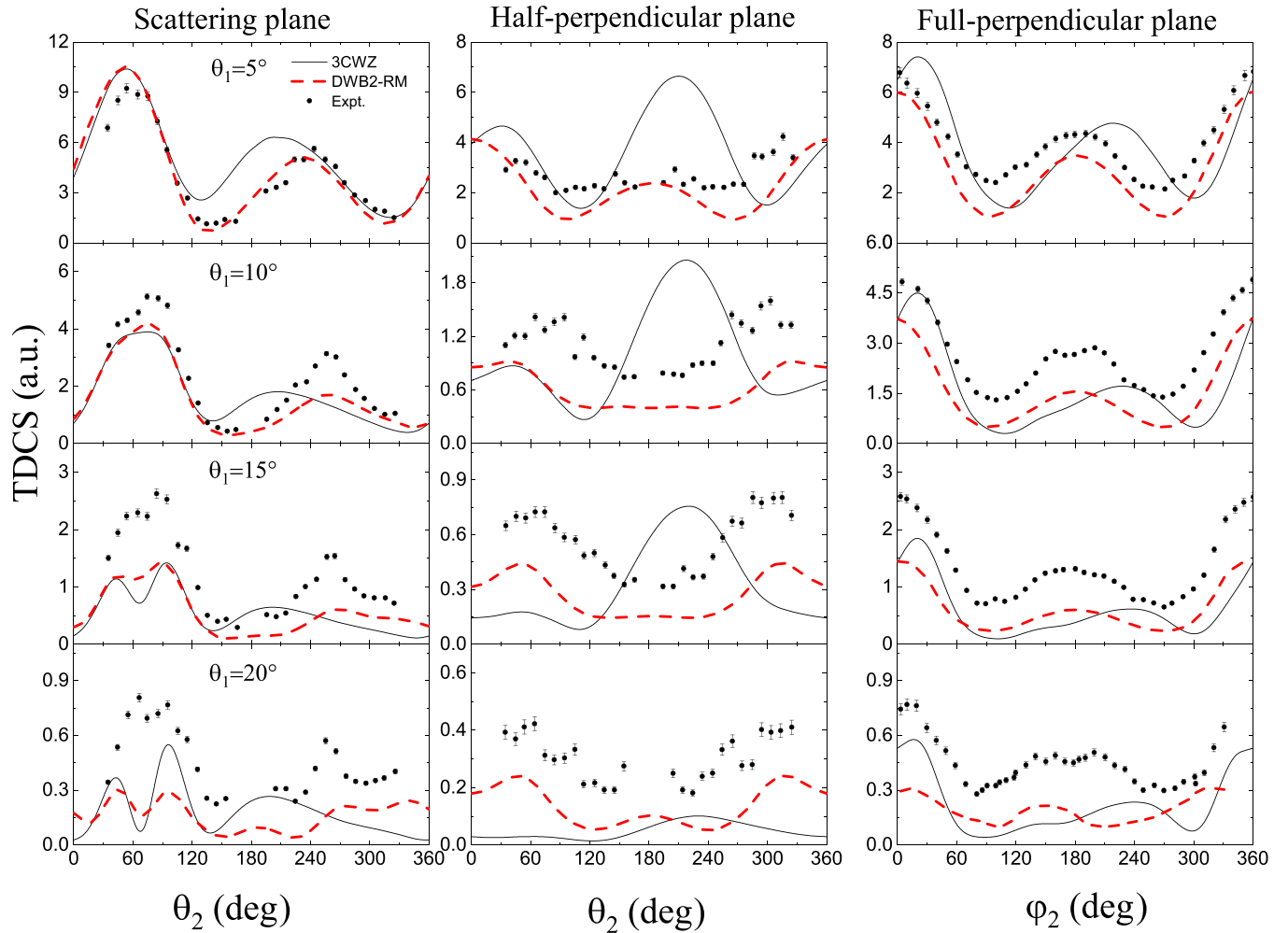


FIG. 6. Same as Fig. 5 but for an ejection energy $E_2 = 15$ eV.

of the PCI which is accounted here and exactly treated. We should note anyway that for highly asymmetric geometries (where PCI may be neglected), DWB2-RM is known to be very efficient.

In summary, for all ejection energies, our modeling reproduces the TDCS in the scattering (xz) plane quite well; a double binary peak appears gradually with increasing scattering angles, in rather better agreement with the data than DWB2-RM. In the out-of-plane geometries, 3CWZ turns out to be less efficient, especially in the half-perpendicular plane (yz plane) in the recoil region, where a strong peak quite far from experiments is observed for all scattering angles. In the full-perpendicular plane (xy plane) both the 3CWZ and DWB2-RM models are able to describe the reaction in some particular kinematics. While DWB2-RM reproduces the data at 10 eV ejection energy quite well, especially at low scattering angles, 3CWZ is much better at describing the TDCS at higher ejection energies (15 and 20 eV), where the data are closer to 3CWZ results for all scattering angles.

IV. CONCLUSION

In this work, an ($e, 2e$) theoretical study of argon 3*p* has been reported in asymmetric kinematics. A 3CWZ model,

based upon a full Coulomb wave description with variable charges, has been used to investigate the ($e, 2e$) ionization reaction in several kinematics; obtained results have been compared with experiments and other theoretical predictions. In a first step, coplanar asymmetric geometry has been considered. At relatively high impact energy (nearly 700 eV) and large momentum transfer (up to 1.6 a.u.) where ejection and scattering energies are rather close, 3CWZ results turned out to be in good agreement with the relative data much better than DWB2-RM. Unlike the previous case (Fig. 3), the agreement with absolute experiments at 200 and 113.5 eV impact energies was found to be rather mixed at lower impact energies and lower momentum transfer (Fig. 4), noting anyway that 3CWZ results were at the same level of agreement with the data as other sophisticated models. In a second step we considered an alternative type of experiment reported on an absolute scale, where the TDCS is presented as a three-dimensional image as a function of the ejection solid angle; comparisons with TDCS cuts in three orthogonal planes are hence made for a series of kinematics. Overall, 3CWZ results are in poor agreement with the data in the half-perpendicular (yz) plane. In the scattering (xz) and the full-perpendicular (xy) planes, on the other hand, results based upon the 3CWZ model seem to agree better with experiments. In the xz plane

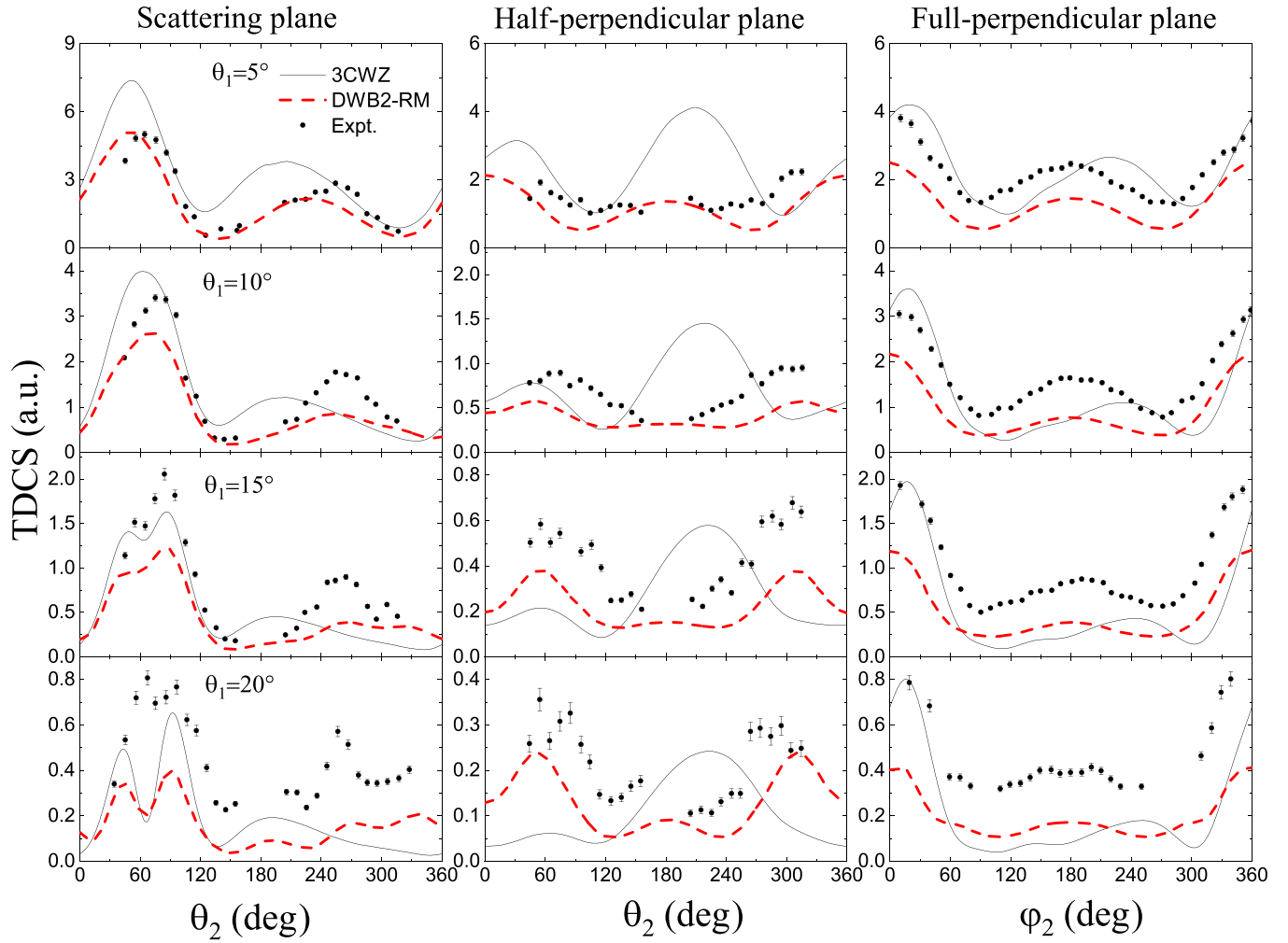


FIG. 7. Same as Fig. 5 but for an ejection energy $E_2 = 20$ eV.

the agreement with the data is quite satisfying and in much better agreement than the rather powerful DWB2-RM model. In the xy plane both theoretical models are able to well reproduce the data in some kinematics.

Given the shortcomings observed in this work the method should be applied for other atoms and in other kinematics [45] for a more exhaustive interpretation of the ionization process. This modeling represents a kind of a full approximated distorted wave approach with PCI, whose advantage is justified by significant savings in computing time. This thereby enables its application to molecular targets which represent actually a great challenge for theory. In fact, theoretical investigations of $(e, 2e)$ for molecules remain relatively scarce due to its multicenter nature as well as the random orientation of the

molecule; the advancement of theoretical models also depends on the availability of reliable experiments for purposes of comparison. Despite all the experimental difficulties, some valuable data are now available for molecules in a range of various kinematics [46,47]; we are able to generalize our 3CWZ to molecules for a more detailed analysis of the $(e, 2e)$ process.

ACKNOWLEDGMENT

This work was supported by the Direction Générale de la Recherche Scientifique et du Développement Technologique (DGRSDT-Algeria), PRFU Grant No. B00L02UN190120200003.

- [1] A. Lahmam-Bennani, *J. Phys. B* **24**, 2401 (1991).
- [2] S. J. Cavanagh and B. Lohmann, *J. Phys. B* **32**, L261 (1999).
- [3] R. El Mir, K. Kaja, A. Naja, E. M. Staicu Casagrande, S. Houamer, and C. Dal Cappello, *J. Phys. B* **54**, 015201 (2021).
- [4] D. H. Madison and O. Al-Hagan, *J. At., Mol., Opt. Phys.* **2010**, 367180 (2010).

- [5] D. H. Madison, R. V. Calhoun, and W. N. Shelton, *Phys. Rev. A* **16**, 552 (1977).
- [6] J. Rasch, C. T. Whelan, R. J. Allan, S. P. Lucey, and H. R. J. Walters, *Phys. Rev. A* **56**, 1379 (1997).
- [7] M. A. Stevenson, L. R. Hargreaves, B. Lohmann, I. Bray, D. V. Fursa, K. Bartschat, and A. Kheifets, *Phys. Rev. A* **79**, 012709 (2009).

- [8] F. K. Miller, C. T. Whelan, and H. R. J. Walters, *Phys. Rev. A* **91**, 012706 (2015).
- [9] A. Prideaux and D. H. Madison, *Phys. Rev. A* **67**, 052710 (2003).
- [10] J. Gao, D. H. Madison, and J. L. Peacher, *Phys. Rev. A* **72**, 020701(R) (2005).
- [11] J. Gao, D. H. Madison, and J. L. Peacher, *J. Chem. Phys.* **123**, 204314 (2005).
- [12] S. Jones and D. H. Madison, *J. Phys. B* **27**, 1423 (1994).
- [13] S. Amami, M. Ulu, Z. N. Ozer, M. Yavuz, S. Kazgoz, M. Dogan, O. Zatsarinny, K. Bartschat, and D. Madison, *Phys. Rev. A* **90**, 012704 (2014).
- [14] H. Chaluvadi, Z. N. Ozer, M. Dogan, C. Ning, J. Colgan, and D. H. Madison, *J. Phys. B* **48**, 155203 (2015).
- [15] P. Descouvemont and D. Baye, *Rep. Prog. Phys.* **73**, 036301 (2010).
- [16] K. Bartschat and P. G. Burke, *J. Phys. B* **20**, 3191 (1987).
- [17] K. Bartschat and P. G. Burke, *J. Phys. B* **21**, 2969 (1988).
- [18] Y. Fang and K. Bartschat, *J. Phys. B* **34**, L19 (2001).
- [19] K. Bartschat and O. Vorov, *Phys. Rev. A* **72**, 022728 (2005).
- [20] I. Bray and A. T. Stelbovics, *Phys. Rev. A* **46**, 6995 (1992).
- [21] I. Bray, *Phys. Rev. Lett.* **89**, 273201 (2002).
- [22] O. Zatsarinny and K. Bartschat, *Phys. Rev. A* **85**, 062709 (2012).
- [23] X. Ren, T. Pflüger, J. Ullrich, O. Zatsarinny, K. Bartschat, D. H. Madison, and A. Dorn, *Phys. Rev. A* **85**, 032702 (2012).
- [24] K. Jung, E. Schubert, D. A. L. Paul, and H. Ehrhardt, *J. Phys. B* **8**, 1330 (1975).
- [25] M. Cherid, A. Lahmam-Bennani, A. Duguet, R. W. Zuraes, R. R. Lucchese, M. C. Dal Cappello, and C. Dal Cappello, *J. Phys. B* **22**, 3483 (1989).
- [26] D. S. Milne-Brownlie, S. J. Cavanagh, B. Lohmann, C. Champion, P. A. Hervieux, and J. Hanssen, *Phys. Rev. A* **69**, 032701 (2004).
- [27] N. Isik, M. Dogan, and S. Bahcelli, *J. Phys. B* **49**, 065203 (2016).
- [28] J. Ullrich, R. Moshhammer, A. Dorn, R. Dörner, L. Ph. H. Schmidt, and H. Schmidt-Böcking, *Rep. Prog. Phys.* **66**, 1463 (2003).
- [29] T. N. Rescigno, M. Baertschy, W. A. Isaacs, and C. W. McCurdy, *Science* **286**, 2474 (1999).
- [30] R. L. Hargreaves, M. A. Stevenson, and B. Lohmann, *J. Phys. B* **43**, 205202 (2010).
- [31] A. Lahmam-Bennani, H. F. Wellenstein, A. Duguet, and A. Daoud, *Phys. Rev. A* **30**, 1511 (1984).
- [32] M. Stevenson, G. J. Leighton, A. Crowe, K. Bartschat, O. K. Vorov, and D. H. Madison, *J. Phys. B* **38**, 433 (2005).
- [33] G. Purohit and D. Kato, *Phys. Rev. A* **96**, 042710 (2017).
- [34] X. Ren, A. Senftleben, T. Pflüger, A. Dörn, K. Bartschat, and J. Ullrich, *J. Phys. B* **43**, 035202 (2010).
- [35] M. Attia, S. Houamer, T. Khatir, K. Bechane, and C. Dal Cappello, *J. Phys. B* **56**, 075201 (2023).
- [36] M. Chinoune, S. Houamer, C. Dal Cappello, and A. Galstyan, *J. Phys. B* **49**, 205201 (2016).
- [37] T. Khatir, S. Houamer, and C. Dal Cappello, *J. Phys. B* **52**, 245201 (2021).
- [38] C. Clementi and C. Roetti, *At. Data Nucl. Data Tables* **14**, 177 (1974).
- [39] J. B. Furness and I. E. McCarthy, *J. Phys. B* **6**, 2280 (1973).
- [40] N. T. Padial and D. W. Norcross, *Phys. Rev. A* **29**, 1742 (1984).
- [41] F. Catoire, E. M. Staicu-Casagrande, M. Nekkab, C. Dal Cappello, K. Bartschat, and A. Lahmam-Bennani, *J. Phys. B* **39**, 2827 (2006).
- [42] A. Kheifets, A. Naja, E. M. Staicu Casagrande, and A. Lahmam Bennani, *J. Phys. B* **41**, 145201 (2008).
- [43] A. J. Murray, N. J. Bowering, and F. H. Read, *J. Phys. B* **33**, 2859 (2000).
- [44] X. Ren, A. Senftleben, T. Pflüger, A. Dorn, K. Bartschat, and J. Ullrich, *Phys. Rev. A* **83**, 052714 (2011).
- [45] X. Ren, S. Amami, O. Zatsarinny, T. Pflüger, M. Weyland, W. Y. Baek, H. Rabus, K. Bartschat, D. Madison, and A. Dorn, *Phys. Rev. A* **91**, 032707 (2015).
- [46] M. Gong, X. Li, S. B. Zhang, S. Niu, X. Ren, E. Wang, A. Dorn, and X. Chen, *Phys. Rev. A* **98**, 042710 (2018).
- [47] E. Wang, X. Ren, M. Gong, E. Ali, Z. Wang, C. Ma, D. Madison, X. Chen, and A. Dorn, *Phys. Rev. A* **102**, 062813 (2020).